JOURNAL OF VIROLOGY, Oct. 2000, p. 9115–9124 Vol. 74, No. 19
0022-538X/00/$04.00+0

The LMP2A ITAM Is Essential for Providing B Cells with Development and Survival Signals In Vivo

MARK MERCHANT, ROBERT G. CALDWELL, AND RICHARD LONGNECKER*

Department of Microbiology-Immunology, Northwestern University Medical School, Chicago, Illinois 60611

Received 23 March 2000/Accepted 5 July 2000

In Epstein-Barr virus-transformed B cells, known as lymphoblastoid cell lines (LCLs), LMP2A binds the tyrosine kinases Syk and Lyn, blocking B-cell receptor (BCR) signaling and viral lytic replication. SH2 domains in Syk mediate binding to a phosphorylated immunoreceptor tyrosine-based activation motif (ITAM) in LMP2A. Mutation of the LMP2A ITAM in LCLs eliminates Syk binding and allows for full BCR signaling, thereby delineating the significance of the LMP2A-Syk interaction. In transgenic mice, LMP2A causes a developmental alteration characterized by a block in surface immunoglobulin rearrangement resulting in BCR-negative B cells. Normally B cells lacking cognate BCR are rapidly apoptosed; however, LMP2A transgenic B cells develop and survive without a BCR. When bred into the recombinase activating gene 1 null ($RAG^{-/-}$) background, all LMP2A transgenic lines produce BCR-negative B cells that develop and survive in the periphery. These data indicate that LMP2A imparts developmental and survival signals to B cells in vivo. In this study, LMP2A ITAM mutant transgenic mice were generated to investigate whether the LMP2A ITAM is essential for the survival phenotype in vivo. LMP2A ITAM mutant B cells develop normally, although transgene expression is comparable to that in previously described nonmutated LMP2A transgenic B cells. Additionally, LMP2A ITAM mutant mice are unable to promote B-cell development or survival when bred into the $RAG^{-/-}$ background or when grown in methylcellulose containing interleukin-7. These data demonstrate that the LMP2A ITAM is required for LMP2A-mediated developmental and survival signals in vivo.

Epstein-Barr virus (EBV) is a ubiquitous human oncogenic herpesvirus associated with a number of proliferative diseases. In lymphoid cell types, EBV causes infectious mononucleosis in naive adolescents and is associated with African Burkitt's lymphoma, Hodgkin's lymphoma, and adult T-cell leukemia (40, 49). Furthermore, individuals with congenital or immune deficiencies often develop EBV-associated lymphoproliferative diseases (66, 81). In the oral epithelia, EBV is associated with nasopharyngeal carcinoma and oral hairy leukoplakia (4, 35, 63, 71). EBV has also been found in smooth muscle tumors and in assorted lung, breast, gastric, and salivary carcinomas; however, it is unclear what role the virus plays in these cancers (2, 3, 11, 27, 31, 32, 43, 45, 64).

The ability for the virus to remain latent within host B cells is a hallmark of EBV infection. During latency, EBV expresses a set of nine well-studied viral proteins. Six proteins are termed Epstein-Barr nuclear antigens (EBNAs), which include EBNA1, EBNA2, EBNA3A, EBNA3B, EBNA3C, and EBNALP (40, 49). The remaining three proteins are the latent membrane proteins 1 (LMP1), LMP2A, and LMP2B (40). B cells transformed by EBV in vitro, termed lymphoblastoid cell lines (LCLs), express all of these proteins, whereas most EBV-related malignancies express only EBNA1, LMP1, and LMP2A (65). In contrast to these cell types, primary B cells from healthy individuals latently infected with EBV express a very limited number of viral proteins, with LMP2A being the most consistently detected transcript (1, 12, 20, 61, 74). While EBNA1 has been shown to be necessary for maintaining the viral episome (40, 80), LMP2A is thought to be important for maintaining viral latency but not viral transformation (22, 48, 52–55, 57–59).

LMP2A consists of a long amino-terminal tail, 12 membrane-spanning domains, and a short carboxy-terminal tail which aggregates in patches on the surface of latently infected cells (22, 23, 50, 51, 58, 68). The amino-terminal tail of LMP2A contains eight constitutively phosphorylated tyrosine residues and several proline-rich regions which are critical for the ability of LMP2A to interact with cellular proteins (22, 24, 25, 57–59). Phosphorylation at tyrosine 112 is important for association between LMP2A and the protein tyrosine kinase (PTK) Lyn (25). Similarly, phosphorylation at tyrosines 74 and 85 of LMP2A, two key regulatory residues in the immunoreceptor tyrosine-based activation motif (ITAM) of LMP2A, allows for association and activation of the Syk PTK (24). Recent evidence has suggested that ubiquitin ligases, such as Nedd4 and AIP4, associate with the proline-rich PY motifs within LMP2A in a phosphorylation-independent manner (37). These LMP2A-cellular protein associations enable LMP2A to block B-cell antigen receptor (BCR) cross-linking in LCLs, leading to a model in which LMP2A maintains both B-cell quiescence and viral latency.

To establish LMP2A as being critical for maintaining EBV latency in vivo, we generated transgenic mice which express LMP2A downstream of the μ immunoglobulin (Ig) heavy-chain enhancer and promoter (Eμ) (6, 7). Analysis of several lines of these EμLMP2A transgenic mice has revealed that two distinct LMP2A in vivo phenotypes exist. Two lines of mice display an $LMP2A^{BCR-}$ phenotype, best characterized by transgenic line E (TgE), while three independent lines of animals display an $LMP2A^{BCR+}$ phenotype, best typified by transgenic line 6 (Tg6). $E\mu LMP2A^{BCR-}$ transgenic lines have been shown by quantitative PCR to express more LMP2A-specific message than $E\mu LMP2A^{BCR+}$ transgenic lines. However, since there are no data addressing the timing of transgene expression in each line during the B-cell developmental time line, these animals are currently considered to represent two distinct phenotypic variants. $E\mu LMP2A^{BCR-}$ transgenic mice

* Corresponding author. Mailing address: Department of Microbiology-Immunology, Northwestern University Medical School, 303 E. Chicago Ave., Chicago, IL 60611. Phone: (312) 503-0467. Fax: (312) 503-1339. E-mail: r-longnecker@nwu.edu.

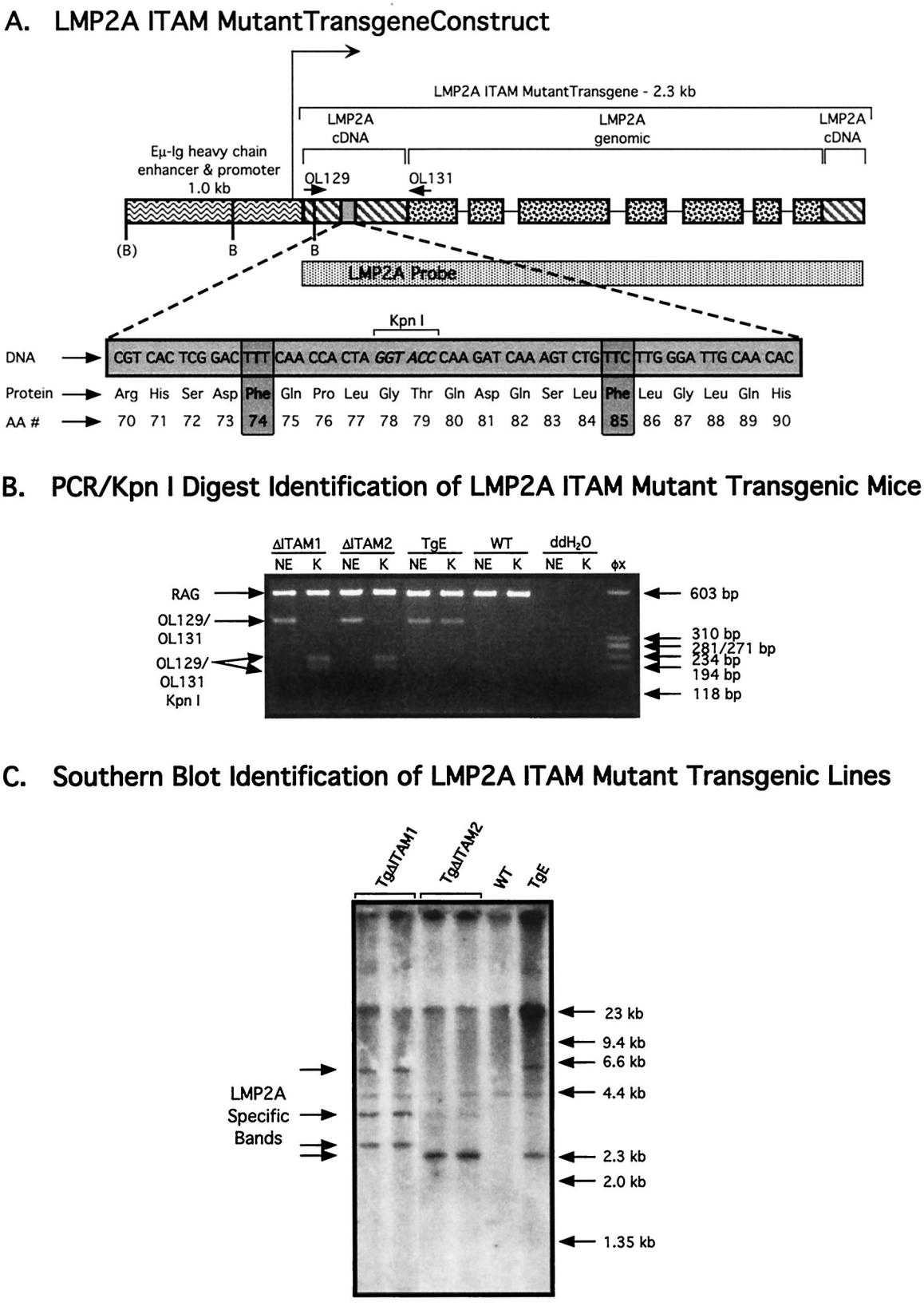

FIG. 1. Generation of LMP2A ITAM mutant transgenic mice. (A) LMP2A ITAM mutant transgene construct. The Eμ heavy-chain enhancer/promoter (wavy lines) was fused to the LMP2A ITAM mutant transgene containing both LMP2A cDNA sequences (striped lines) and EBV genomic sequences (stippled). The DNA, protein, and amino acid number (AA #) for the altered ITAM sequences are shown in the shaded inset at the bottom. A silent point mutation creates a *Kpn*I site in the LMP2A ITAM mutant transgene, which aids in distinguishing ITAM mutant mice from LMP2A transgenic mice by PCR using OL129 and OL131 (upper inset) followed by

display a B-cell developmental alteration characterized by a bypass of Ig heavy-chain rearrangement resulting in an overall loss of surface Ig (sIg) expression. PCR amplification of Ig gene rearrangements in EμLMP2A^{BCR-} transgenic bone marrow cells demonstrated that rearrangement of the D-J_H heavy chain and V-J_K light-chain genes occurs correctly; however, there is a failure to complete the final V-DJ_H rearrangement of the heavy chain. B cells that lose a functioning BCR have been shown to rapidly undergo apoptosis (44). Nonetheless, EμLMP2A^{BCR-} B cells are capable of exiting the bone marrow and persisting in the periphery. EμLMP2A^{BCR+} lines display a less prominent phenotype consisting of slight decreases in mature B-cell numbers, while the resulting B cells appear largely normal. When bred into a RAG-1-deficient (RAG$^{-/-}$) background, both EμLMP2A^{BCR-} and EμLMP2A^{BCR+} lines are capable of producing B cells that exit the bone marrow and persist in the periphery. These observations were supported by the growth of RAG$^{-/-}$ EμLMP2A bone marrow cells in methylcellulose containing interleukin-7 (IL-7). These data indicate that LMP2A drives B-cell development and survival in the absence of normal BCR signals.

In this study, we used an LMP2A ITAM mutant, encoding mutations of tyrosines 74 and 85 to phenylalanines [Y(74/85)F], to create EμLMP2A ΔITAM transgenic mice. Generation of these mice allows for investigation of whether the in vivo developmental and survival signals observed in LMP2A transgenic mice derive from the LMP2A ITAM. These mice show no B-cell developmental alteration or survival phenotype in any B-cell compartment. Furthermore, this transgene is incapable of driving B-cell development or survival when bred into the RAG$^{-/-}$ background in vivo or when grown in methylcellulose in vitro. These data show that LMP2A must have a functional ITAM in order to enhance B-cell development and survival. These results suggest that Syk activation by a phosphorylated ITAM is required for LMP2A to provide developmental and survival signals in vivo.

MATERIALS AND METHODS

Mice. Constructions of the EμLMP2A transgene and LMP2A ITAM mutant [Y(74/85)F] have been previously described (7, 24). The LMP2A ΔITAM mutant transgene containing the double mutation Y(74/85)F was constructed as follows. The *Eco*RI-*Sal*I DNA fragment from pRH38, coding for the Y(74/85)F mutant amino-terminal tail of LMP2A, was cloned into *Mun*I-*Sal*I-digested pRL202, which codes for the Eμ enhancer and promoter transgene construct, to generate pRG3. The *Msc*I-*Xho*I fragment from pRL209, which codes for the remainder of the LMP2A transgene, was inserted into *Msc*I-*Xho*I-digested pRG3 to generate pRG4. The *Sac*I-*Xho*I fragment of pRG4 containing the Eμ promoter/enhancer and LMP2A ΔITAM transgene was used for standard microinjection into (B6 × CBA)F_1 single-cell fertilized eggs as described elsewhere (36). The resulting offspring were screened by PCR and Southern blotting for the presence of LMP2A. The identified founders were bred to C57BL/6 or RAG$^{-/-}$ animals in the BL/6 background for all described experiments. The animals were housed at the Northwestern University Center for Experimental Animal Resources in accordance with university animal welfare guidelines. Wild-type C57BL/6 and RAG$^{-/-}$ animals were obtained from Jackson Laboratories.

Tail DNA isolation. DNA was prepared as previously described (6, 7). Briefly, a 1-cm piece of tail was digested in a 1.5-ml microcentrifuge tube overnight in 500 μl of tail lysis buffer (100 mM Tris [pH 8], 100 mM NaCl, 5 mM EDTA, 0.2% sodium dodecyl sulfate [SDS], 100 μg of proteinase K/ml) at 55°C. Digested tail lysates were vortexed and centrifuged for 10 min, and supernatants were transferred to a new 1.5-ml microcentrifuge tube. Supernatants were precipitated with 2 volumes of 95% ethanol and centrifuged at 4°C for 20 min; DNA pellets were air dried and resuspended in 200 μl of Tris-EDTA.

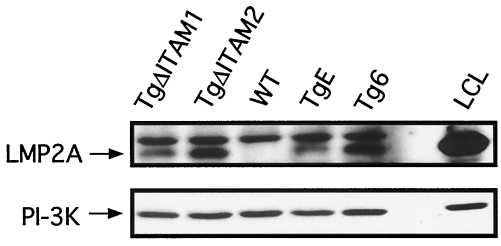

FIG. 2. LMP2A expression in LMP2A ITAM mutant transgenic lines is similar to that in nonmutated LMP2A transgenic mice. Immunoblot analyses of LMP2A and p85 expression in splenic tissues from TgΔITAM1, TgΔITAM2, WT, TgE, and Tg6 animals are shown. The LMP2A and p85 subunit (PI-3K) bands are indicated by arrows. LMP2A-expressing EBV-transformed LCLs served as a positive control.

Southern hybridization. Ten micrograms of mouse genomic tail DNA was digested overnight at 37°C with *Bam*HI (1× NEB [New England Biolabs] *Bam*HI buffer, 1× bovine serum albumin [BSA], 20 U of *Bam*HI [NEB]) and electrophoresed on a 0.8% agarose gel. The gel was then treated sequentially with 0.25 N HCl for 10 min and 0.4 M NaOH for 30 min followed by transfer of the gel onto GeneScreen Plus (NEN) using a vacuum blotter (Appligene). LMP2A probe was generated by digesting the LMP2A cDNA clone pRL34 with *Eco*RI, releasing the 2.0-kb cDNA in its entirety, followed by gel purification, ethanol precipitation, and resuspension to 20 ng/μl. Then 1.0 μl (20 ng) of this DNA was labeled with [α-^{32}P]dCTP (Amersham-Pharmacia) using Ready-to-Go (-dCTP) labeling beads (Amersham-Pharmacia) followed by a purification step to remove unincorporated [α-^{32}P]dCTP, using G-50 Probe-Quant spin columns (Amersham-Pharmacia) according to the manufacturers recommendations. The blot was prehybridized for 1 h at 68°C in 30 ml of hybridization solution (6× SSC [0.9 M NaCl, 0.09 M sodium citrate], 1× Denhardt's solution [0.02% BSA, 0.02% Ficoll, 0.02% polyvinylpyrrolidine], 62.5 mM Tris [pH 7.5], 0.05% SDS) with 100 μg of denatured herring sperm DNA per ml. Roughly 10^6 cpm of labeled probe was denatured and added directly to 10 ml of 68°C hybridization solution; the blot was added, and the solution was allowed to hybridize overnight at 68°C. Following hybridization, the blot was washed according to the following regimen: twice with 2× SSC at room temperature, twice with 2× SSC–1% SDS, and twice with 0.1× SSX–1% SDS. The blot was then wrapped in Saran Wrap and exposed to film.

PCR. PCR for the presence of the LMP2A transgene was done as previously described (6, 7). Briefly, each 25.0-μl reaction mixture contained 1× PCR buffer (Pharmacia), 0.2 mM each deoxynucleoside triphosphate, 1.0 U of *Taq* polymerase (Pharmacia), 1 μM each oligonucleotide primer, 1× PCR cresol red loading dye (60% sucrose, 5 mM cresol red [Sigma]), and 1.0 μl of genomic tail DNA. The amplification cycle (15 s at 94°C, 30 s at 58°C, and 75 s at 72°C) was repeated 30 times, followed by a single 10-min extension at 72°C. A unique silent *Kpn*I site was engineered between residues 74 and 85 to distinguish LMP2A ΔITAM mutant animals from nonmutated LMP2A transgenic animals (Fig. 1A). LMP2A amino-terminal primers (OL129 and OL131) were designed to amplify the region of LMP2A containing the engineered *Kpn*I site. These primers were used, in combination with RAG internal control primers, in a PCR followed by overnight digestion with *Kpn*I (1× NEB buffer 1, 1× BSA, 25.0 μl of PCR mixture, 1.0 U of *Kpn*I [NEB]) at 37°C. The oligonucleotide primers not previously described are as follows: LMP2A amino-terminal primer pair (370 bp), OL129 (TGGGTACGATGGCGGAAACAACTC) and OL131 (TGAAACACGAGGC GGCAATAGC); RAG (180 bp), OL107 (TGACTGTGGGAACTGCTGAAC TTT) and OL138 (CCGTGGACGCTAAAACCCAAAGTC); and Neo (280 bp), Neo-2 (CAACAGACAATCGGCTGCTCTGATG) and Neo-3 (CATTGC ATCAGCCATGATGGA).

Protein isolation. Spleens were dissected from animals, homogenized between the frosted edges of two microscope slides, and suspended into 10 ml of ice-cold 1× phosphate-buffered saline (PBS). Samples were centrifuged at 1,500 rpm for 10 min, supernatants were poured off, and red blood cells were lysed in 5 ml of red blood cell lysis buffer (150 mM NH_4Cl, 17 mM Tris base [pH 7.2]) for 5 min. Cell suspensions were added to 5 ml of ice-cold 1× PBS through a nylon mesh. Bone marrow methylcellulose samples were prepared by washing methylcellulose cultures with 10 ml of 1× PBS, centrifuging them at 1,500 rpm for 10 min, and resuspending them in 10 ml of 1× PBS. Following cell counting, samples were

*Kpn*I digestion. The LMP2A cDNA probe shown spans sequences throughout the LMP2A transgene. *Bam*HI (B) sites are indicated. The *Bam*HI site in parentheses may be lost upon integration. (B) PCR/*Kpn*I digest identification of LMP2A ITAM mutant transgenic mice. Tail genomic DNA sequences from LMP2A ITAM mutant, nonmutated LMP2A, and WT littermate control animals were amplified using OL129-OL131 and RAG positive control primers, followed by digestion with *Kpn*I (K) or no enzyme (NE). Identities of the amplified products and their subsequent digested fragments are shown to the left. ϕX DNA digested with *Hae*III was used as a size standard (right-most lane). (C) Southern hybridization analysis of LMP2A ITAM mutant lines. Tail DNAs from TgΔITAM1, TgΔITAM2, TgE, and WT animals were digested with *Bam*HI, run on an 0.8% agarose gel, and probed for LMP2A sequences by Southern hybridization. Size standards are indicated at the right.

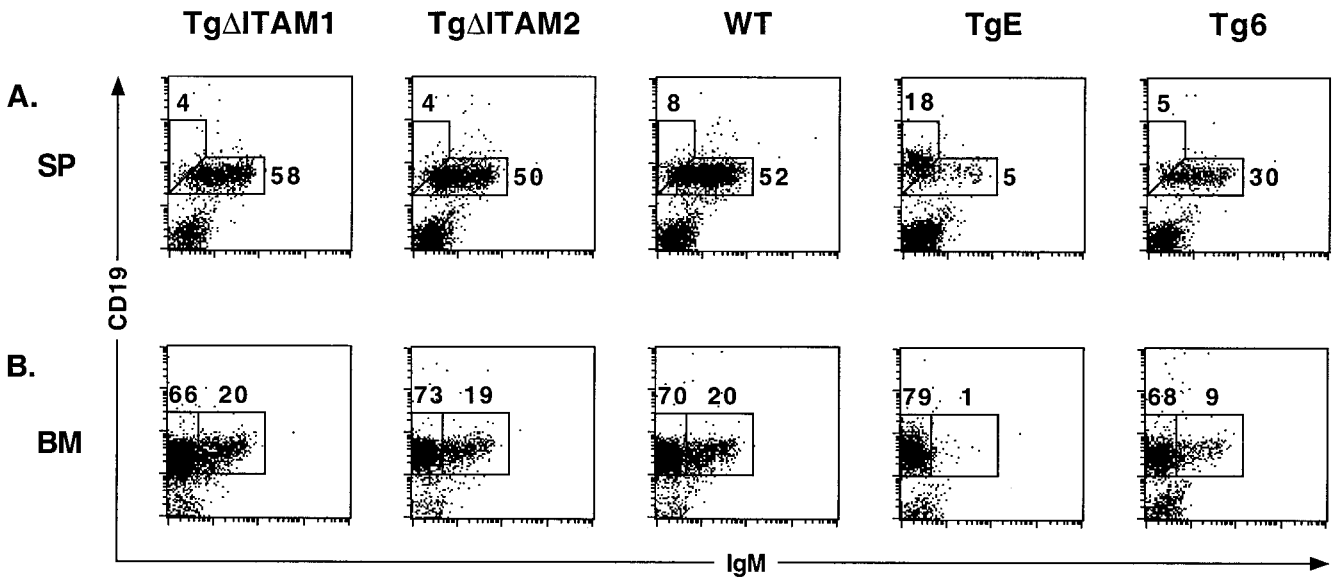

FIG. 3. TgΔITAM1 and TgΔITAM2 mice show no B-cell developmental defect. (A) Spleen (SP) tissues were immunostained with CD19-PE and IgM-FITC antibodies; flow cytometry dot plots are shown. Two distinct cell types are highlighted with boxes, and the respective percentages of gated cells within those regions are denoted. (B) Bone marrow (BM) cells were immunostained as above; the boxes highlight pre-B and mature B cells, and the respective percentages within those regions are denoted.

centrifuged at 1,500 rpm for 5 min, and cell pellets were lysed with the addition of enough Triton X lysis buffer (1% Triton X-100, 20 mM Tris [pH 8.0], 137 mM NaCl, 10% glycerol, 2 mM EDTA, 1 mM sodium vanadate, 10 mM sodium fluoride, 1× phenylmethylsulfonyl fluoride, 1× pepstatin, 1× leupeptin) to bring samples to 200×10^6 cells/ml for spleen samples or 100×10^6 cells/ml for methylcellulose samples. Lysates were allowed to rotate at 4°C for 15 min before being vortexed and cleared of nonsoluble proteins by centrifugation three times for 20 min. Cleared lysates were mixed 1:1 with 2× SDS sample buffer (150 mM Tris-HCl [pH 6.8], 2% SDS, 2% glycerol, 1.43 M β-mercaptoethanol) before being loaded.

Immunoblotting. For immunoblot analysis, 2.5×10^6 cell equivalents of spleen cell equivalents and 0.25×10^6 cell equivalents of control LCLs were heated at 70°C for 10 min, loaded onto a 1.5 mM 7% polyacrylamide gels, and run at 100 V for 1.5 h. Gels were electroblotted to Immobilon-P (Millipore) according to the manufacturer's recommendations. Blots were stained with Ponceau S reagent (Sigma) to ensure equal loading and then blocked in 4% milk in 1× TBST (10 mM Tris [pH 8.0], 150 mM NaCl, 0.05% Tween 20) for 1 h at room temperature. Blots were then washed once for 15 min and twice for 5 min each with 1× TBST. Rat monoclonal anti-LMP2A antibody (14B7-1-1; 2.8 μg/ml) or rabbit anti-phosphatidylinositol 3-kinase (PI3-K) p85 antibody (1 μg/ml; Upstate Biotechnology) was diluted in 1% milk–1× TBST to 1:2,500 and 1:5,000, respectively, and allowed to incubate with blots overnight at 4°C. Blots were again washed once for 15 min and twice for 5 min each with 1× TBST. Horseradish peroxidase (HRP)-conjugated goat anti-rat (Jackson ImmunoResearch Laboratories) or HRP-conjugated sheep anti-rabbit (New England Biolabs) secondary antibodies were diluted in 1× TBST to 1:10,000 and 1:5,000, respectively, and added to the appropriate blots for 30 min at room temperature. Blots were washed once for 15 min and four times for 5 min each with 1× TBST followed by detection with Western blotting Luminol reagent (Santa Cruz Biotechnology, Inc.) according to manufacturer's recommendations; the blots were exposed to film.

Flow cytometry. Spleens were dissected from animals, homogenized between the frosted edges of two microscope slides, and suspended into 10 ml of ice-cold FACS (fluorescence-activated cell sorting) buffer (1× PBS, 10 mM HEPES, 1% fetal calf serum, 0.01% sodium azide). The femurs and tibia were dissected from mice, and the bone marrow was rinsed out into 15-ml tubes with a total of 10 ml of ice-cold serum-free RPMI 1640 (Gibco). Spleen samples were centrifuged at 1,500 rpm for 10 min, and supernatants were poured off. The splenic red blood cells were lysed in 5 ml of red blood cell lysis buffer (150 mM NH_4Cl, 17 mM Tris base [pH 7.2]) for 5 min and were then added to 5 ml of ice-cold FACS buffer through a nylon mesh. Following cell counting, samples were centrifuged at 1,500 rpm for 5 min, and cells were resuspended to 40×10^6/ml in ice-cold FACS buffer; 2×10^6 cells per spleen stain or 4×10^6 cells per bone marrow stain were used in 100 μl of antibody stains. Samples were incubated with 0.5 μg of Fc block (Pharmingen) per stain for 15 min at 4°C, followed by addition of staining antibodies for 30 min at 4°C in the dark. The following antibody dilutions were made in FACS buffer and used in various combinations to stain cells: IgM-fluorescein isothiocyanate (FITC) (1:60) and CD19-phycoerythrin (PE) (1:1,200). Following staining, samples were washed once in 2 ml of 1× PBS and were routinely fixed in 1% paraformaldehyde–1× PBS at 4°C overnight in the dark. All antibodies were purchased from Pharmingen. Samples were run on a Becton Dickinson FACScan, and data were analyzed using CellQuest software.

Methylcellulose cultures. Bone marrow cells were collected in serum-free RPMI 1640 as outlined above, counted, centrifuged at 1,500 rpm for 10 min, and resuspended to 10×10^6/ml. A total of 2×10^6 bone marrow cells were seeded in 3 ml of murine preB Methocult containing IL-7 (Stem Cell Technologies). Cells were vortexed for 30 s to evenly distribute cells in the methylcellulose and then evenly plated into two 60-mm-diameter dishes according to the manufacturer's recommendations. Cultures were grown for 7 days at 37°C in 5% CO_2. Colonies were photographed and scored for morphology and number before being harvested for use in flow cytometry and immunoblots.

RESULTS

Generation of LMP2A ITAM mutant transgenic mice. The EμLMP2A Y(74/85)F mutant ITAM transgene was constructed as outlined in Materials and Methods, released from the parent plasmid by digestion with *Sac*I and *Xho*I, purified, and microinjected into $(B6 \times CBA)F_1$ mouse oocytes. From these injections, 12 offspring were produced, 2 of which were found to be transgenic by PCR (see Materials and Methods) and designated TgΔITAM1 and TgΔITAM2.

Founder DNA was subjected to restriction enzyme and sequence analysis to determine whether the newly constructed transgenic lines contained the proper mutated sequences. The Y(74/85)F ITAM mutant LMP2A sequence contains an engineered silent point mutation creating a unique *Kpn*I site in the amino-terminal portion of the transgene (Fig. 1A), enabling ITAM mutant founders to be distinguished from previously described nonmutated LMP2A transgenic mice. Genomic tail DNA from the TgΔITAM1 founder, the TgΔITAM2 founder, an LMP2A transgenic line E (TgE) animal, and a wild-type (WT) littermate control animal were subjected to PCR using primers OL129 and OL131, amplifying the amino-terminal portion of LMP2A containing the unique *Kpn*I site. Following PCR amplification, the reactions were subjected to digestion with *Kpn*I or an equivalent reaction with no enzyme. DNA from both TgΔITAM1 and TgΔITAM2 produced PCR products of 370 bp, equal to those produced in nonmutated LMP2A transgenic mice (Fig. 1B). When these products were digested

with *Kpn*I, only products from TgΔITAM1 and TgΔITAM2 were digested to produce two smaller products of 197 and 173 bp; PCR products from TgE remained undigested (Fig. 1B). These data show that the TgΔITAM1 and TgΔITAM2 animals contain the expected *Kpn*I site engineered into the transgene. Sequence analysis of OL129-OL131 PCR products from each line confirmed the presence of the expected sequence in each line (data not shown).

LMP2A sequence was detected in *Bam*HI-digested genomic tail DNAs from TgΔITAM1, TgΔITAM2, TgE, and WT littermate control animals by Southern blot analysis (Fig. 1C). Each transgenic sample hybridizes to LMP2A-specific bands, indicating the presence of the transgenes in each line. These hybridization patterns have been stable for over four generations (data not shown).

LMP2A is expressed similarly in LMP2A ITAM mutant transgenic lines and nonmutated LMP2A transgenic mice. B-cell transgene expression was detected in TgΔITAM1 and TgΔITAM2 splenocytes by immunoblot analysis. Whole spleen lysates from age-matched 4- to 8-week-old TgΔITAM1, TgΔITAM2, TgE, Tg6, and WT control animals were immunoblotted using an anti-LMP2A antibody (14B7-1-1) and an antibody against the p85 subunit of PI-3K, to control for loading. TgΔITAM1 and TgΔITAM2 express LMP2A to similar levels as both TgE and Tg6 animals (Fig. 2). A higher nonspecific band is consistently seen in all mouse samples tested but not in the human LCL positive control lane, presumably due to cross-reactivity of the secondary goat anti-rat HRP-labeled antibody with mouse proteins. Blots were stripped and immunoblotted against PI-3K to show that protein loading was roughly equivalent in all lanes. No obvious differences in onset of transgene expression or in the general pattern described above were observed when expression was tested in young animals (data not shown).

LMP2A ITAM mutant transgenic mice display no B-cell developmental alteration. Spleen and bone marrow samples from TgΔITAM1 and TgΔITAM2 were analyzed by flow cytometry to determine whether LMP2A ITAM mutant mice display a B-cell developmental phenotype similar to that seen in previously described nonmutated LMP2A lines TgE and Tg6. Spleen and bone marrow samples from each transgenic line as well as WT littermate controls were analyzed by flow cytometry for mouse sIgM (IgM-FITC) and the pan-B-cell marker CD19 (CD19-PE) (Fig. 3). WT animals displayed normal levels of $CD19^+$ IgM^+ B cells in the spleen (52%) and bone marrow (20%). In contrast, TgE animals displayed the previously reported developmental alteration, characterized by a severe reduction in the numbers of $CD19^+$ IgM^+ B cells in the spleen (5%) and bone marrow (1%). Similarly, Tg6 animals showed the previously reported phenotype of slight decreases in the numbers of $CD19^+$, IgM^+ B-cell numbers in the spleen (30%) and bone marrow (9%). Both TgΔITAM1 and TgΔITAM2 mice displayed no B-cell developmental defects and had no significant differences in the spleen (58 and 50% versus 52%, respectively) or bone marrow (20 and 19% versus 20%, respectively) compared to WT littermate controls. No defects were observable in any T-cell compartment in either LMP2A ΔITAM mutant or nonmutated LMP2A transgenic mice (data not shown).

LMP2A ITAM mutant mice cannot support development or survival in the $RAG^{-/-}$ background. Previous reports have divided LMP2A transgenic animals into $E\mu LMP2A^{BCR-}$ and $E\mu LMP2A^{BCR+}$ classes (6, 7). $E\mu LMP2A^{BCR-}$ transgenic mice can be clearly distinguished by loss of IgM expression on their B cells when analyzed by flow cytometry. However, the $E\mu LMP2A^{BCR+}$ transgenic B cells appear similar to their WT littermate controls by the same analysis. When both classes of LMP2A transgenics are bred into the $RAG^{-/-}$ background, both have a readily observable phenotype. $RAG^{-/-}$ animals are unable to rearrange Ig genes to form Ig, the key protein of the BCR, thus blocking B-cell development at the pre-B cell stage. This results in a complete absence of mature B cells in $RAG^{-/-}$ animal bone marrow and peripheral lymphoid organs. When bred into the $RAG^{-/-}$ background, both classes of LMP2A transgenic animals generate a greater number of $CD19^+$ B cells in the bone marrow and peripheral lymphoid organs. These data indicate that LMP2A imparts a developmental and survival signal in all classes of LMP2A transgenic animals.

To determine whether the TgΔITAM1 and TgΔITAM2 proteins could provide B cells with developmental or survival signals in the absence of RAG-1, both lines were bred into the $RAG^{-/-}$ background. Spleen and bone marrow samples were prepared from $RAG^{-/-}$ TgΔITAM1, $RAG^{-/-}$ TgΔITAM2, $RAG^{-/-}$ TgE, $RAG^{-/-}$ Tg6, and $RAG^{-/-}$ control animals for analysis by flow cytometry. Both $RAG^{-/-}$ TgE and $RAG^{-/-}$ Tg6 animals show enhanced survival of B cells, as indicated by the accumulation of $CD19^{hi+}$ B cells in the spleen (25 and 2%, respectively) as well as an increase in CD19 expression in the bone marrow (Fig. 4). In contrast to these results, neither $RAG^{-/-}$ TgΔITAM1 nor $RAG^{-/-}$ TgΔITAM2 animals show any enhancement of CD19 expression or B-cell survival in the spleen or bone marrow and are indistinguishable from $RAG^{-/-}$ littermate controls.

LMP2A ITAM mutant transgenic bone marrow cells grow comparably to WT littermate controls in methylcellulose containing IL-7. Growth of bone marrow cells in methylcellulose medium containing IL-7 has allowed for an additional measure of the developmental effect of LMP2A on B cells. When bone marrow cells from TgΔITAM1, TgΔITAM2, TgE, Tg6, and WT littermates were cultured for 7 days in methylcellulose medium, each line produced B-cell colonies (Fig. 5A). Cells collected from methylcellulose cultures from each transgenic line were subjected to flow cytometry analysis (Fig. 5B). The B-cell outgrowths from these cultures reflect the general trend observed in bone marrow samples in vivo. TgE methylcellulose cultures are predominantly (98%) $CD19^+$ IgM^-, while Tg6 methylcellulose cultures show a slight reduction in the number of $CD19^+$ IgM^+ cells (11% versus 30%) and an increase in the number of $CD19^+$ IgM^- (88% versus 68%) compared to WT controls. In contrast, both TgΔITAM1 and TgΔITAM2 methylcellulose cultures contain similar percentages of $CD19^+$ IgM^+ (31 and 26% versus 30%, respectively) and $CD19^+$ IgM^- (65 and 70% versus 68%, respectively) cells compared to WT cultures (Fig. 5B). The number of B-cell colonies formed in each plate correlates with the strength of the developmental and survival signal that LMP2A imparts. TgE bone marrow produces nearly twice as many colonies on average (Student's *t* test, $P = 0.0017$) compared to TgΔITAM1, TgΔITAM2, and WT littermate controls (Fig. 5C). These data represent counts collected from four separate experiments in which Tg6 bone marrow was not cultured and is therefore not represented in the graph. These results indicate that TgΔITAM1 and TgΔITAM2 mutant LMP2A protein does not provide any colony-forming enhancement signal as seen in nonmutated LMP2A transgenic bone marrow when cultured in vitro.

In the $RAG^{-/-}$ background, the LMP2A ITAM mutant transgene is unable to support development or survival of bone marrow cells in methylcellulose. When bone marrow from any $RAG^{-/-}$ LMP2A transgenic mouse is cultured in methylcellulose media, a substantial enhancement of colony number can be observed (6, 7). Therefore, $RAG^{-/-}$

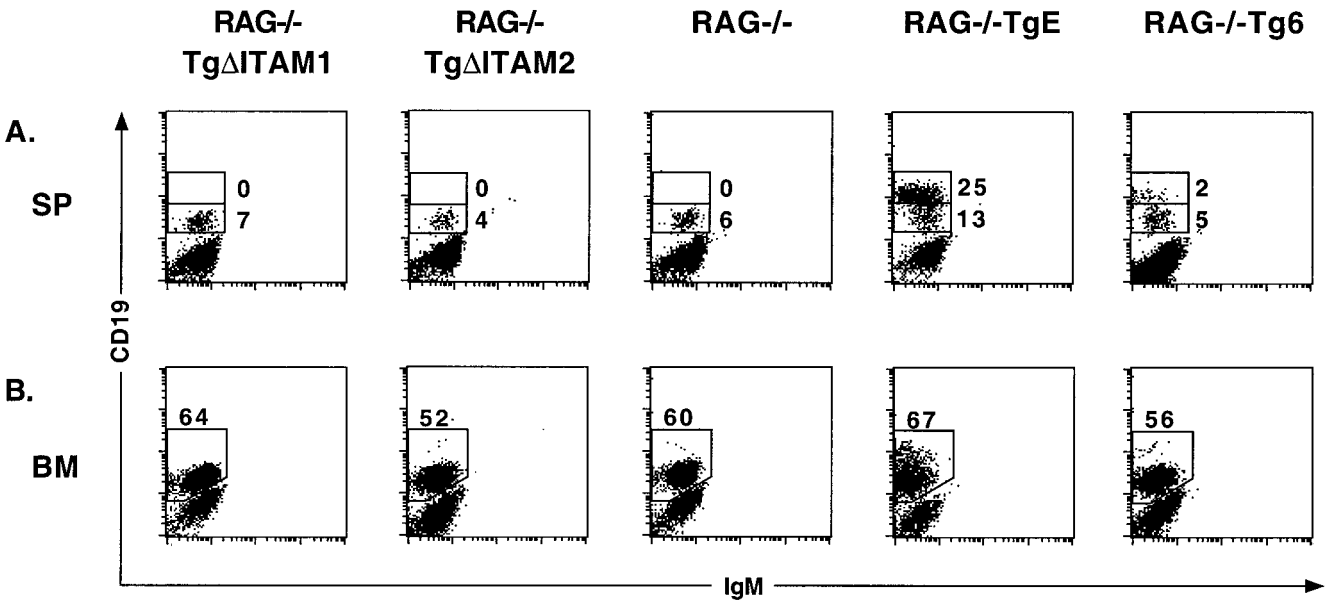

FIG. 4. LMP2A ITAM mutant mice do not impart a survival signal to RAG$^{-/-}$ B cells. (A) Spleen (SP) tissues were immunostained with CD19-PE and IgM-FITC antibodies; flow cytometry dot plots are shown. Two distinct cell types are highlighted with boxes in the plots, and the respective percentages of gated cells within those regions are denoted. (B) Bone marrow (BM) cells were immunostained as above; the boxed inset shows the percentage of CD19^{+} cells arising in the bone marrow, and the respective percentages of gated cells within those regions are denoted.

TgΔITAM1, RAG$^{-/-}$ TgΔITAM2, RAG$^{-/-}$ TgE, RAG$^{-/-}$ Tg6, and RAG$^{-/-}$ littermate control bone marrow samples were cultured in IL-7-containing methylcellulose. As expected, both RAG$^{-/-}$ TgE and RAG$^{-/-}$ Tg6 bone marrow cultures generated significant numbers of colonies in methylcellulose (Fig. 5D). Both RAG$^{-/-}$ TgΔITAM1 and RAG$^{-/-}$ TgΔITAM2 did not form any significant numbers of colonies, similar to their RAG$^{-/-}$ littermate control animals. Flow cytometry analysis of recovered RAG$^{-/-}$ TgE and RAG$^{-/-}$ Tg6 bone marrow cells showed that nearly all were CD19^{+} IgM^{-} as expected (data not shown). Too few cells were recovered from RAG$^{-/-}$ TgΔITAM1, RAG$^{-/-}$ TgΔITAM2, and RAG$^{-/-}$ animals to determine surface marker phenotype. These results show that TgΔITAM1 and TgΔITAM2 animals lack any LMP2A-derived developmental or survival signal.

DISCUSSION

Both in vitro and in vivo systems have been used to determine the function of LMP2A in EBV latency. In vitro studies using EBV-transformed LCLs have shown that LMP2A is highly tyrosine phosphorylated and forms aggregates in the plasma membrane of latently infected cells. Associated with LMP2A are the Src family PTKs, the Syk PTK, and Nedd4 family ubiquitin ligases (24, 25, 37, 57). Of particular interest to these studies is the specific association of the LMP2A ITAM with the Syk PTK (24). In vitro, these LMP2A protein complexes result in a complete block in BCR-mediated signal transduction (24, 25, 57, 58). In vivo studies have provided additional information into LMP2A function. In transgenic mice, LMP2A provides both developmental and survival signals to B lymphocytes (6, 7).

This study was designed to determine the importance of the LMP2A ITAM in the LMP2A-mediated developmental and survival signal observed in the previously described LMP2A transgenic mice (6, 7). Comparing ITAM defective LMP2A transgenic mice with the previously constructed LMP2A transgenic lines, we demonstrate the importance of the LMP2A ITAM in providing the LMP2A-mediated developmental and survival signal. Previous studies have described two distinct LMP2A transgenic phenotypes. Two of five genetically distinct LMP2A lines have a dramatic phenotype (LMP2A^{BCR-}) characterized by the development and survival of B lymphocytes lacking a BCR in an immunocompetent murine background (7). Three other lines exhibit a more subtle phenotype (LMP2A^{BCR+}) when analyzed in an immunocompetent background. However, when all LMP2A transgenic animals are bred into the RAG-null background, LMP2A allows for both the developmental and survival of B lymphocytes in peripheral immune organs (6, 7).

In this study, we analyzed two different LMP2A ITAM mutant transgenic lines, both of which were unable to promote B-cell development or survival in either an immunocompetent or RAG-null background. Although it is possible that these ITAM-defective LMP2A lines may not express enough LMP2A to generate the previously characterized LMP2A phenotypes, this seems unlikely for two reasons. First, as demonstrated, both ITAM-defective lines generated in this study express approximately equal levels of LMP2A protein in B lymphocytes compared to the previously described LMP2A transgenic lines. Second, of the five nonmutated LMP2A transgenic lines analyzed to date, all have the developmental and survival phenotype when bred into the RAG-null background.

The requirement for an intact LMP2A ITAM to provide B cells with a developmental and survival signal in vivo implicates Syk as being a major target for LMP2A. Many studies have demonstrated a vital role for Syk in B-cell development and activation (13, 73, 76). Syk$^{-/-}$ mice display perinatal lethality, indicating that Syk plays a vital role in organismal development (13, 76). However, when irradiated WT mice are reconstituted with fetal liver cells from Syk$^{-/-}$ mice, the reconstituted lymphoid cells exhibit a severe B-cell developmental phenotype. These mice are characterized by a block of B-cell development at the pro-B-to-pre-B cell transition, resulting in a lack of

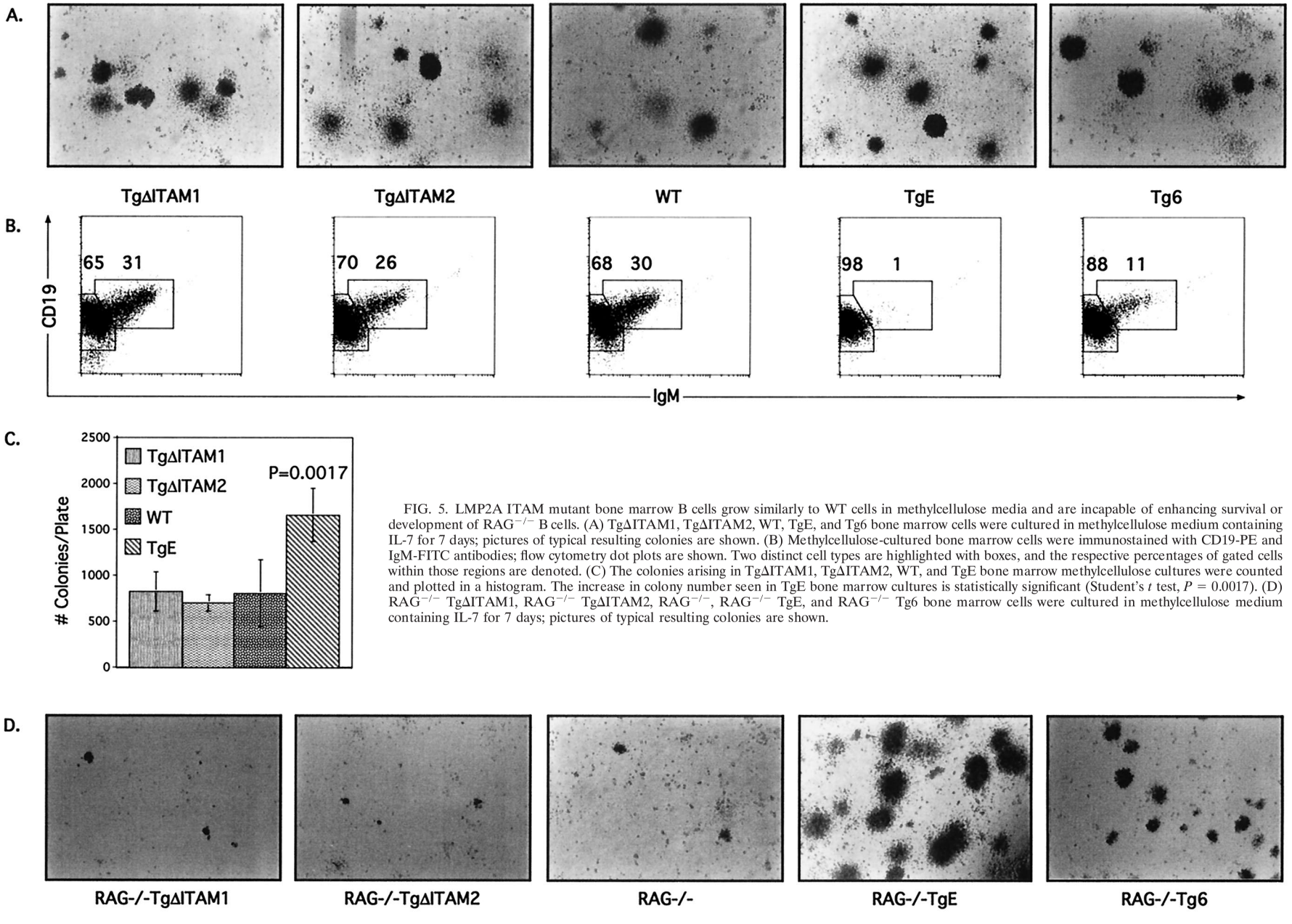

FIG. 5. LMP2A ITAM mutant bone marrow B cells grow similarly to WT cells in methylcellulose media and are incapable of enhancing survival or development of $RAG^{-/-}$ B cells. (A) TgΔITAM1, TgΔITAM2, WT, TgE, and Tg6 bone marrow cells were cultured in methylcellulose medium containing IL-7 for 7 days; pictures of typical resulting colonies are shown. (B) Methylcellulose-cultured bone marrow cells were immunostained with CD19-PE and IgM-FITC antibodies; flow cytometry dot plots are shown. Two distinct cell types are highlighted with boxes, and the respective percentages of gated cells within those regions are denoted. (C) The colonies arising in TgΔITAM1, TgΔITAM2, WT, and TgE bone marrow methylcellulose cultures were counted and plotted in a histogram. The increase in colony number seen in TgE bone marrow cultures is statistically significant (Student's t test, $P = 0.0017$). (D) $RAG^{-/-}$ TgΔITAM1, $RAG^{-/-}$ TgΔITAM2, $RAG^{-/-}$, $RAG^{-/-}$ TgE, and $RAG^{-/-}$ Tg6 bone marrow cells were cultured in methylcellulose medium containing IL-7 for 7 days; pictures of typical resulting colonies are shown.

mature B cells as well as a partial impairment of T-cell development.

Syk has been firmly established as a critical factor for the generation of both the Ca^{2+} influx and mitogen-activated protein kinase (MAPK) signals that follow BCR cross-linking (for reviews, see references 8, 41, and 42). For production of the Ca^{2+} response, Syk is critical for phosphorylation and activation of a number of downstream targets, including PI-3K, BLNK, and phospholipase γ2 (PLC-γ2) (10, 26, 38, 73). Following sIg cross-linking, Syk phosphorylates and activates PI-3K, which initiates the production of biologically active phosphoinositides that act as second messengers (16, 21). Interestingly, activation of PI-3K is also critical for activation of the antiapoptotic protein Akt, which may be a target for LMP2A in enhancing cell survival (17, 29). Btk associates with the PI-3K product phosphatidylinositol-3,4,5-trisphosphate [$PI(3,4,5)P_3$], allowing for autophosphorylation and activation (47, 69, 78). Phosphorylated BLNK has been shown to provide docking sites for downstream signaling molecules, thus allowing them to aggregate and become activated (26). BLNK binds both activated Btk and PLC-γ2, thus allowing Btk and Syk to phosphorylate and activate PLC-γ2 (19, 33, 38, 72). Once activated, PLC-γ2 mediates the production of diacylglycerol and inositol trisphosphate from the PI-3K product $PI(4,5)P_2$ (34). Diacylglycerol is critical for activation of protein kinase C, whereas inositol trisphosphate causes a release of Ca^{2+} from intracellular stores (56, 62). Influx of Ca^{2+} leads to activation of the calmodulin-dependent protein kinase II and the calmodulin-activated serine/theonine phosphatase calcineurin (70, 77). One of the factors activated by an influx of calcium is the transcription factor NF-AT, which is important for upregulation of a number of cytokines and immune effector molecules (15, 79).

A more direct generation of MAPK signals by Syk downstream of the BCR has also been well established. BLNK phosphorylation by Syk leads to binding of guanine nucleotide exchange factors Vav and the Grb2 and Nck adapter proteins through SH2-phosphotyrosine associations (26). Docking of these effectors to BLNK allow for activation of the Ras and Rac GTPases (5, 9, 18, 46). Phosphorylation cascades though the ERK, JNK, and p38 arms of the MAPK pathways result in activation of a number of transcription factors such as Fos, Jun, and members of the Ets family (14, 30, 60, 75). Studies using Syk-null DT40 chicken B cells have shown that Syk is critical for activation of the ERK1 and JNK1 arms of the MAPK family (39).

The LMP2A ITAM mutant mouse data suggest that LMP2A may be manipulating Syk to direct the activation of a MAPK- and/or a Ca^{2+}-mediated signal in order to enhance B-cell survival and maintain latency. In so doing, LMP2A may be mimicking a constitutively active BCR or a docking protein, such as BLNK, thus directing signals away from the actual BCR while replacing the essential signals normally arising from a functional BCR with LMP2A-derived survival signals. Future studies will map the pathways downstream of the LMP2A ITAM-Syk interaction critical for LMP2A to block BCR signal transduction and produce survival signals. Of particular interest are pathways that lead to activation or upregulation of antiapoptotic proteins such as Akt. Other signaling proteins acting downstream of Syk that are important for B-cell development, such as Btk and BLNK, also clearly warrant further study using our transgenic mouse models. These studies should provide a clearer understanding of the transmission of LMP2A signals and how these signals affect B-cell development, survival, and EBV latency.

ACKNOWLEDGMENTS

R.L. is supported by Public Health Service grants CA62234 and CA73507 from the National Cancer Institute and DE13127 from the National Institute of Dental and Craniofacial Research. R.L. is a Scholar of the Leukemia Society of America.

We are grateful for the contributions from members of the Longnecker and Spear laboratories at Northwestern University.

REFERENCES

1. **Babcock, G. J., L. L. Decker, M. Volk, and D. A. Thorley-Lawson.** 1998. EBV persistence in memory B cells in vivo. Immunity **9:**395–404.
2. **Begin, L. R., J. Eskandari, J. Joncas, and L. Panasci.** 1987. Epstein-Barr virus related lymphoepithelioma-like carcinoma of lung. J. Surg. Oncol. **36:**280–283.
3. **Bonnet, M., J. M. Guinebretiere, E. Kremmer, V. Grunewald, E. Benhamou, G. Contesso, and I. Joab.** 1999. Detection of Epstein-Barr virus in invasive breast cancers. J. Natl. Cancer Inst. **91:**1376–1381.
4. **Bouzid, M., D. Djennaoui, J. Dubreuil, A. Bouguermouh, D. Ellouz, J. Abdelwahab, G. Decaussin, and T. Ooka.** 1994. Epstein-Barr virus genotypes in NPC biopsies from North Africa. Int. J. Cancer **56:**468–473.
5. **Buday, L., S. E. Egan, V. P. Rodriguez, D. A. Cantrell, and J. Downward.** 1994. A complex of Grb2 adaptor protein, Sos exchange factor, and a 36-kDa membrane-bound tyrosine phosphoprotein is implicated in ras activation in T cells. J. Biol. Chem. **269:**9019–9023.
6. **Caldwell, R. G., R. C. Brown, and R. Longnecker.** 2000. Epstein-Barr virus LMP2A-induced B-cell survival in two unique classes of EμLMP2A transgenic mice. J. Virol. **74:**1101–1113.
7. **Caldwell, R. G., J. B. Wilson, S. J. Anderson, and R. Longnecker.** 1998. Epstein-Barr virus LMP2A drives B cell development and survival in the absence of normal B cell receptor signals. Immunity **9:**405–411.
8. **Campbell, K. S.** 1999. Signal transduction from the B cell antigen-receptor. Curr. Opin. Immunol. **11:**256–264.
9. **Cantrell, D.** 1998. Lymphocyte signalling: a coordinating role for Vav? Curr. Biol. **8:**R535–R538.
10. **Carter, R. H., D. J. Park, S. G. Rhee, and D. T. Fearon.** 1991. Tyrosine phosphorylation of phospholipase C induced by membrane immunoglobulin in B lymphocytes. Proc. Natl. Acad. Sci. USA **88:**2745–2749.
11. **Chan, J. K., T. T. Yip, W. Y. Tsang, Y. F. Poon, C. S. Wong, and V. W. Ma.** 1994. Specific association of Epstein-Barr virus with lymphoepithelial carcinoma among tumors and tumorlike lesions of the salivary gland. Arch. Pathol. Lab. Med. **118:**994–997.
12. **Chen, F., J. Z. Zou, and L. di Renzo.** 1995. A subpopulation of normal B cells latently infected with Epstein-Barr virus resembles Burkitt lymphoma cells in expressing EBNA-1 but not EBNA-2 or LMP1. J. Virol. **69:**3752–3758.
13. **Cheng, A. M., B. Rowley, W. Pao, A. Hayday, J. B. Bolen, and T. Pawson.** 1995. Syk tyrosine kinase required for mouse viability and B-cell development. Nature **378:**303–306.
14. **Chiles, T. C., J. L. Liu, and T. L. Rothstein.** 1991. Cross-linking of surface Ig receptors on murine B lymphocytes stimulates the expression of nuclear tetradecanoyl phorbol acetate-response element-binding proteins. J. Immunol. **146:**1730–1735.
15. **Choi, M., R. D. Brines, M. J. Holman, G. G. Klaus.** 1994. Induction of NF-AT in normal B lymphocytes by anti-immunoglobulin or CD40 ligand in conjunction with IL-4. Immunity **1:**179–187.
16. **Corvera, S., and M. P. Czech.** 1998. Direct targets of phosphoinositide 3-kinase products in membrane traffic and signal transduction. Trends Cell Biol. **8:**442–446.
17. **Craxton, A., A. Jiang, T. Kurosaki, and E. A. Clark.** 1999. Syk and Bruton's tyrosine kinase are required for B cell antigen receptor-mediated activation of the kinase Akt. J. Biol. Chem. **274:**30644–30650.
18. **Crespo, P., X. R. Bustelo, D. S. Aaronson, O. A. Coso, M. Lopez-Barahona, M. Barbacid, and J. S. Gutkind.** 1996. Rac-1 dependent stimulation of the JNK/SAPK signaling pathway by Vav. Oncogene **13:**455–460.
19. **DeBell, K. E., B. A. Stoica, M. C. Veri, A. Di Baldassarre, S. Miscia, L. J. Graham, B. L. Rellahan, M. Ishiai, T. Kurosaki, and E. Bonvini.** 1999. Functional independence and interdependence of the Src homology domains of phospholipase C-γ1 in B-cell receptor signal transduction. Mol. Cell. Biol. **19:**7388–7398.
20. **Decker, L. L., L. D. Klaman, and D. A. Thorley-Lawson.** 1996. Detection of the latent form of Epstein-Barr virus DNA in the peripheral blood of healthy individuals. J. Virol. **70:**3286–3286.
21. **Duronio, V., M. P. Scheid, and S. Ettinger.** 1998. Downstream signalling events regulated by phosphatidylinositol 3-kinase activity. Cell Signal. **10:** 233–233.
22. **Fruehling, S., R. Caldwell, and R. Longnecker.** 1997. LMP2 function in EBV Latency. EBV Rep. **4:**141–159.
23. **Fruehling, S., S. K. Lee, R. Herrold, B. Frech, G. Laux, E. Kremmer, F. A. Grasser, and R. Longnecker.** 1996. Identification of latent membrane protein 2A (LMP2A) domains essential for the LMP2A dominant-negative effect on B-lymphocyte surface immunoglobulin signal transduction. J. Virol. **70:**6216–6226.

24. **Fruehling, S., and R. Longnecker.** 1997. The immunoreceptor tyrosine-based activation motif of Epstein-Barr virus LMP2A is essential for blocking BCR-mediated signal transduction. Virology **235:**241–251.
25. **Fruehling, S., R. Swart, K. M. Dolwick, E. Kremmer, and R. Longnecker.** 1998. Tyrosine 112 of latent membrane protein 2A is essential for protein tyrosine kinase loading and regulation of Epstein-Barr virus latency. J. Virol. **72:**7796–7806.
26. **Fu, C., C. W. Turck, T. Kurosaki, and A. C. Chan.** 1998. BLNK: a central linker protein in B cell activation. Immunity **9:**93–103.
27. **Fukayama, M., Y. Hayashi, Y. Iwasaki, J. Chong, T. Ooba, T. Takizawa, M. Koike, S. Mizutani, M. Miyaki, and K. Hirai.** 1994. Epstein-Barr virus-associated gastric carcinoma and Epstein-Barr virus infection of the stomach. Lab. Investig. **71:**73–81.
28. **Ghaffari-Tabrizi, N., B. Bauer, A. Villunger, G. Baier-Bitterlich, A. Altman, G. Utermann, F. Uberall, and G. Baier.** 1999. Protein kinase Cθ, a selective upstream regulator of JNK/SAPK and IL-2 promoter activation in Jurkat T cells. Eur. J. Immunol. **29:**132–142.
29. **Gold, M., M. P. Scheid, L. Santos, M. Dang-Lawson, R. A. Roth, L. Matsuuchi, V. Duronio, and D. L. Krebs.** 1999. The B cell antigen receptor activates the Akt (protein kinase B)/glycogen synthase kinase-3 signaling pathway via phosphatidylinositol 3-kinase. J. Immunol. **163:**1894–1905.
30. **Grant, P. A., C. B. Thompson, and S. Pettersson.** 1995. IgM receptor-mediated transactivation of the IgH 3′ enhancer couples a novel Elf-1-AP-1 protein complex to the developmental control of enhancer function. EMBO J. **14:**4501–4513.
31. **Gulley, M. L., D. R. Pulitzer, P. A. Eagan, and B. G. Schneider.** 1996. Epstein-Barr virus infection is an early event in gastric carcinogenesis and is independent of bcl-2 expression and p53 accumulation. Hum. Pathol. **27:**20–27.
32. **Harn, H. J., L. I. Ho, W. H. Chung, J. J. Lin, H. S. Lee, and W. H. Lee.** 1995. Epstein-Barr virus-associated typical gastric carcinoma detected by in situ hybridization and polymerase chain reaction. J. Clin. Gastroenterol. **20:**253–254.
33. **Hashimoto, S., A. Iwamatsu, M. Ishiai, K. Okawa, T. Yamadori, M. Matsushita, Y. Baba, T. Kishimoto, T. Kurosaki, and S. Tsukada.** 1999. Identification of the SH2 domain binding protein of Bruton's tyrosine kinase as BLNK—functional significance of Btk-SH2 domain in B-cell antigen receptor-coupled calcium signaling. Blood **94:**2357–2364.
34. **Hempel, W. M., R. C. Schatzman, and A. L. DeFranco.** 1992. Tyrosine phosphorylation of phospholipase C-gamma 2 upon cross-linking of membrane Ig on murine B lymphocytes. J. Immunol. **148:**3021–3027.
35. **Hitt, M. M., M. J. Allday, T. Hara, L. Karran, M. D. Jones, P. Busson, T. Tursz, I. Ernberg, and B. E. Griffin.** 1989. EBV gene expression in an NPC-related tumour. EMBO J. **8:**2639–2651.
36. **Hogan, B., R. Beddington, F. Constantini, and E. Lacy.** 1994. Manipulating the mouse embryo, a laboratory manual, 2nd ed. Cold Spring Harbor Laboratory Press, Cold Spring Harbor, N.Y.
37. **Ikeda, M., A. Ikeda, L. C. Longan, and R. Longnecker.** 2000. The Epstein-Barr virus (EBV) latent membrane protein 2A (LMP2A) PY motif recruits WW domain-containing ubiquitin-protein ligases. Virology **268:**178–191.
38. **Ishiai, M., M. Kurosaki, R. Pappu, K. Okawa, I. Ronko, C. Fu, M. Shibata, A. Iwamatsu, A. C. Chan, and T. Kurosaki.** 1999. BLNK required for coupling Syk to PLC gamma 2 and Rac1-JNK in B cells. Immunity **10:**117–125.
39. **Jiang, A., A. Craxton, T. Kurosaki, E. A. Clark.** 1998. Different protein tyrosine kinases are required for B cell antigen receptor-mediated activation of extracellular signal-regulated kinase, c-Jun NH2-terminal kinase 1, and p38 mitogen-activated protein kinase. J. Exp. Med. **188:**1297–1306.
40. **Kieff, E.** 1996. Epstein-Barr virus and its replication, p. 1109–1162. *In* B. N. Fields, D. M. Knipe, and P. M. Howley (ed.), Fundamental virology, Lippincott-Raven, Philadelphia, Pa.
41. **Kurosaki, T.** 1999. Genetic analysis of B cell antigen receptor signaling. Annu. Rev. Immunol. **17:**555–592.
42. **Kurosaki, T.** 1998. Molecular dissection of B cell antigen receptor signaling. Bioorg. Med. Chem. Lett. **1:**515–527.
43. **Labrecque, L. G., D. M. Barnes, I. S. Fentiman, and B. E. Griffin.** 1995. Epstein-Barr virus in epithelial cell tumors: a breast cancer study. Cancer Res. **55:**39–45.
44. **Lam, K., R. Kuhn, and K. Rajewsky.** 1997. In vivo ablation of surface immunoglobulin on mature B cells by inducible gene targeting results in rapid cell death. Cell **90:**1073–1083.
45. **Lanier, A. P., S. R. Clift, G. Bornkamm, W. Henle, H. Goepfert, and N. Raab Traub.** 1991. Epstein-Barr virus and malignant lymphoepithelial lesions of the salivary gland. Arctic Med. Res. **50:**55–61.
46. **Li, N., A. Batzer, R. Daly, V. Yajnik, E. Skolnik, P. Chardin, S. D. Bar, B. Margolis, and J. Schlessinger.** 1993. Guanine-nucleotide-releasing factor hSos1 binds to Grb2 and links receptor tyrosine kinases to Ras signalling. Nature **363:**85–88.
47. **Li, Z., M. I. Wahl, A. Eguinoa, L. R. Stephens, P. T. Hawkins, and O. N. Witte.** 1997. Phosphatidylinositol 3-kinase-gamma activates Bruton's tyrosine kinase in concert with Src family kinases. Proc. Natl. Acad. Sci. USA **94:**13820–13825.
48. **Longnecker, R.** 1994. Biochemical and genetic studies of Epstein-Barr virus latent membrane protein 2. Leukemia **8:**S46–S50.
49. **Longnecker, R.** 1998. Molecular biology of Epstein-Barr virus, p. 133–172. *In* Dennis McCance (ed.), Human tumor viruses, American Society for Microbiology, Washington, D.C.
50. **Longnecker, R., B. Druker, T. M. Roberts, and E. Kieff.** 1991. An Epstein-Barr virus protein associated with cell growth transformation interacts with a tyrosine kinase. J. Virol. **65:**3681–3692.
51. **Longnecker, R., and E. Kieff.** 1990. A second Epstein-Barr virus membrane protein (LMP2) is expressed in latent infection and colocalizes with LMP1. J. Virol. **64:**2319–2326.
52. **Longnecker, R., and C. L. Miller.** 1996. Regulation of Epstein-Barr virus latency by latent membrane protein 2. Trends Microbiol. **4:**38–42.
53. **Longnecker, R., C. L. Miller, X.-Q. Miao, A. Marchini, and E. Kieff.** 1992. The only domain which distinguishes Epstein-Barr virus latent membrane 2A (LMP2A) from LMP2B is dispensable for lymphocyte infection and growth transformation in vitro, and LMP2A is therefore nonessential. J. Virol. **66:**6461–6469.
54. **Longnecker, R., C. L. Miller, X. Q. Miao, B. Tomkinson, and E. Kieff.** 1993. The last seven transmembrane and carboxy-terminal cytoplasmic domains of Epstein-Barr virus latent membrane protein 2 (LMP2) are dispensable for lymphocyte infection and growth transformation in vitro. J. Virol. **67:**2006–2013.
55. **Longnecker, R., C. L. Miller, B. Tomkinson, X. Q. Miao, and E. Kieff.** 1993. Deletion of DNA encoding the first five transmembrane domains of Epstein-Barr virus latent membrane proteins 2A and 2B. J. Virol. **67:**5068–5074.
56. **McConnell, F. M., S. B. Shears, P. J. Lane, M. S. Scheibel, and E. A. Clark.** 1992. Relationships between the degree of cross-linking of surface immunoglobulin and the associated inositol 1,4,5-trisphosphate and Ca^{2+} signals in human B cells. Biochem. J. **284:**447–455.
57. **Miller, C. L., A. L. Burkhardt, J. H. Lee, B. Stealey, R. Longnecker, J. B. Bolen, and E. Kieff.** 1995. Integral membrane protein 2 of Epstein-Barr virus regulates reactivation from latency through dominant negative effects on protein-tyrosine kinases. Immunity **2:**155–166.
58. **Miller, C. L., J. H. Lee, E. Kieff, and R. Longnecker.** 1994. An integral membrane protein (LMP2) blocks reactivation of Epstein-Barr virus from latency following surface immunoglobulin crosslinking. Proc. Natl. Acad. Sci. USA **91:**772–776.
59. **Miller, C. L., R. Longnecker, and E. Kieff.** 1993. Epstein-Barr virus latent membrane protein 2A blocks calcium mobilization in B lymphocytes. J. Virol. **67:**3087–3094.
60. **Mittlestadt, P. R., and A. L. DeFranco.** 1993. Induction of early response genes by cross-linking membrane Ig on B lymphocytes. J. Immunol. **150:**4822–4832.
61. **Miyashita, E. M., B. Yang, G. J. Babcock, and D. A. Thorley-Lawson.** 1997. Identification of the site of Epstein-Barr virus persistence in vivo as a resting B cell. J. Virol. **71:**4882–4891.
62. **Padeh, S., A. Levitzki, A. Gazit, G. B. Mills, and C. M. Roifman.** 1991. Activation of phospholipase C in human B cells is dependent on tyrosine phosphorylation. J. Clin. Investig. **87:**1114–1118.
63. **Raab-Traub, N.** 1992. Epstein-Barr virus and nasopharyngeal carcinoma. Semin. Cancer Biol. **3:**297–307.
64. **Raab-Traub, N., P. Rajadurai, K. Flynn, and A. P. Lanier.** 1991. Epstein-Barr virus infection in carcinoma of the salivary gland. J. Virol. **65:**7032–7036.
65. **Rickinson, A. B., and E. Kieff.** 1996. Epstein-Barr virus, p. 2397–446. *In* B. N. Fields, D. M. Knipe, and P. M. Howley (ed.), Fields virology. Lippincott-Raven Publishers, Philadelphia, Pa.
66. **Riddler, S. A., M. C. Breinig, and J. L. McKnight.** 1994. Increased levels of circulating Epstein-Barr virus (EBV)-infected lymphocytes and decreased EBV nuclear antigen antibody responses are associated with the development of posttransplant lymphoproliferative disease in solid-organ transplant recipients. Blood **84:**972–984.
67. **Sakata, N., H. Kawasome, N. Terada, P. Gerwins, G. L. Johnson, E. W. Gelfand.** 1999. Differential activation and regulation of mitogen-activated protein kinases through the antigen receptor and CD40 in human B cells. Eur. J. Immunol. **29:**2999–3008.
68. **Sample, J., D. Liebowitz, and E. Kieff.** 1989. Two related Epstein-Barr virus membrane proteins are encoded by separate genes. J. Virol. **63:**933–937.
69. **Scharenberg, A., and J. P. Kinet.** 1998. PtdIns-3,4,5-P3: a regulatory nexus between tyrosine kinases and sustained calcium signals. Cell **94:**5–8.
70. **Schreiber, S. L., and G. R. Crabtree.** 1992. The mechanism of action of cyclosporin A and FK506. Immunol. Today **13:**136–142.
71. **Sugihara, K., H. Reupke, A. Schmidt Westhausen, H. D. Pohle, H. R. Gelderblom, and P. A. Reichart.** 1990. Negative staining EM for the detection of Epstein-Barr virus in oral hairy leukoplakia. J. Oral Pathol. Med. **19:**367–370.
72. **Takata, M., and T. Kurosaki.** 1996. A role for Bruton's tyrosine kinase in B cell antigen receptor-mediated activation of phospholipase C-gamma 2. J. Exp. Med. **184:**31–40.
73. **Takata, M., H. Sabe, A. Hata, T. Inazu, Y. Homma, T. Nukada, H. Yamamura, and T. Kurosaki.** 1994. Tyrosine kinases Lyn and Syk regulate B

cell receptor-coupled Ca^{2+} mobilization through distinct pathways. EMBO J. **13:**1341–1349.

74. **Tierney, R. J., N. Steven, L. S. Young, and A. B. Rickinson.** 1994. Epstein-Barr virus latency in blood mononuclear cells: analysis of viral gene transcription during primary infection and in the carrier state. J. Virol. **68:**7374–7385.
75. **Tilzey, J. F., T. C. Chiles, and T. L. Rothstein.** 1991. Jun-B gene expression mediated by the surface immunoglobulin receptor of primary B lymphocytes. Biochem. Biophys. Res. Commun. **175:**77–83.
76. **Turner, M., P. J. Mee, P. S. Costello, O. Williams, A. A. Price, L. P. Duddy, M. T. Furlong, R. L. Geahlen, and V. L. Tybulewicz.** 1995. Perinatal lethality and blocked B-cell development in mice lacking the tyrosine kinase Syk. Nature **378:**298–302.
77. **Valentine, M. A., A. J. Czernik, N. Rachie, H. Hidaka, C. L. Fisher, J. C. Cambier, and K. Bomsztyk.** 1995. Anti-immunoglobulin M activates nuclear calcium/calmodulin-dependent protein kinase II in human B lymphocytes. J. Exp. Med. **182:**1943–1949.
78. **Varnai, P., K. I. Rother, and T. Balla.** 1999. Phosphatidylinositol 3-kinase-dependent membrane association of the Bruton's tyrosine kinase pleckstrin homology domain visualized in single living cells. J. Biol. Chem. **274:**10983–10989.
79. **Venkataraman, L., D. A. Francis, Z. Wang, J. Liu, T. L. Rothstein, and R. Sen.** 1994. Cyclosporin-A sensitive induction of NF-AT in murine B cells. Immunity **1:**189–196.
80. **Yates, J. L., N. Warren, and B. Sugden.** 1985. Stable replication of plasmids derived from Epstein-Barr virus in various mammalian cells. Nature **313:**812–815.
81. **Young, L., C. Alfieri, K. Hennessy, H. Evans, C. O'Hara, K. C. Anderson, J. Ritz, R. S. Shapiro, A. Rickinson, E. Kieff, and J. I. Cohen.** 1989. Expression of Epstein-Barr virus transformation-associated genes in tissues of patients with EBV lymphoproliferative disease. N. Engl. J. Med. **321:**1080–1085.